

## PHOTOSENSITIVITY IN ANTIMONY BASED GLASSES

M. Nalin<sup>a,b</sup>, Y. Messaddeq<sup>a</sup>, S. J. L. Ribeiro<sup>a</sup>, M. Poulain<sup>b</sup>, V. Briois<sup>c</sup>

<sup>a</sup> Laboratório de Materiais Fotônicos, Instituto de Química, UNESP, rua Professor Francisco Degni, Araraquara – SP, Brazil

<sup>b</sup> Laboratoire des Matériaux Photoniques, Université de Rennes 1, Rennes, France

<sup>c</sup> LURE, Université Paris Sud, BP34, 91898 Orsay cedex, France

New glass forming systems based on  $\text{Sb}_2\text{O}_3$ - $\text{SbPO}_4$  has been explored. These glasses present higher thermal stability against devitrification and higher refractive index than chalcogenide glasses. Under irradiation, using Ar-laser 350nm wavelength and 50 mW power density, change on the coloration is observed. Structural and electronic modifications around Sb cations induced by such treatment have been characterized by XANES measurements at the L-Sb edges. On the one hand, XANES spectra, at the  $L_3$  edge, show a decrease of the coordination number for Sb atoms induced by exposure to light indicating a breaking of Sb-O bonds in the glassy network. On the other hand, XANES spectra, at the  $L_1$  edge, suggest a change in the oxidation state of Sb atoms. These modifications associated to the photodarkening of the glass is reversible either after a couple of days or after heating the glass at the glass transition temperature,  $T_g$ .

(Received May 30, 2001; accepted June 11, 2001)

*Keywords:* Antimony based glass, Photosensitivity, XANES method

### 1. Introduction

Heavy metal oxide based glasses have been the subject of several studies [1]. Particularly, antimony oxide glasses have been studied as they present extended infrared transmission [2]. Several studies have been focused on optical properties mainly non linear optical properties as they present higher refractive index [3,4].

Several photoinduced processes have been reported in oxide glasses. It is known as photoexpansion, photodarkening, etc. The phenomenon allows the fabrication of different phase structure as example, the Bragg grating obtained by photoimprinting a periodic index modulation [5,6]. The photosensitivity may led also the fabrication of miniature thin film by directly writing a channel waveguide in a photosensitive wafer without the use of chemical process as photoresist or etching. For oxide systems, in the case of silica glasses a volume change is observed. Several studies are reported on thin film  $\text{Sb}_2\text{S}_3$  in view of its photosensitive and thermoelectric properties [7]. In our Knowledge, no studies are reported in the literature on photoinduced phenomenon on antimony oxide glasses. A photocontraction effect is recently observed on thin film  $\text{Sb}_2\text{S}_3$  under UV irradiation [8]. In this sense antimony based glasses may also be photosensitive under irradiation. One of the reasons that can be considered is the lone pair present in the trivalent antimony ions. The presence of this lone pair in the amorphous network could be accountable for break and formation of bonds during exposure.

This work reports the investigation of new glass compositions which could be photosensitive materials. The structural behaviors of the binary  $\text{Sb}_2\text{O}_3$ - $\text{SbPO}_4$  glass systems before and after irradiation have been particularly studied, using mainly as structural tools the XANES spectroscopy.

### 2. Experimental

#### 2.1. Glass preparation

Starting materials used for glass preparation are  $\text{Sb}_2\text{O}_3$  (Acros 99%) and  $\text{SbPO}_4$ .  $\text{SbPO}_4$  is prepared in the lab by mixing  $\text{Sb}_2\text{O}_3$  and  $\text{H}_3\text{PO}_4$ (85%). Details of this preparation is reported on ref.

[9]. Synthesis were carried out by melting starting materials in glassy carbon crucibles in electrical furnace for 10 minutes at 700-1000 °C. Then the melt was cast and glass samples were obtained upon cooling. For less stable glasses, melt was quenched between two brass pieces, which lead to samples of 1 mm or less in thickness. Sample thickness can reach 10 mm for compositions less prone to devitrification by casting the melt into a brass mould preheated around  $T_g$ . Large samples were annealed around this temperature for two hours to reduce thermal stresses.

## 2.2. Physical measurements

Characteristics temperatures ( $T_g$  for glass transition temperature,  $T_x$  for onset of crystallisation and  $T_p$  for maximum of crystallisation peak) were determined by differential scanning calorimeter (DSC) using a SEIKO SSC/5200H equipment. The estimated error on the temperature is 2 K for glass transition and onset of crystallisation which are obtained from tangents intersection and 1 K for the position of the crystallisation peak. Powdered samples were set in aluminium pans under  $N_2$  atmosphere at 10 K/Min heating rate. Infrared transmission spectra were recorded with a BOMEM Michelson Spectrophotometer in the 400-4000  $cm^{-1}$  range. Ultraviolet transmission spectra between 800 and 200 nm were obtained using a Varian spectrophotometer Cary 5. The irradiation process was performed at LURE (Orsay, France) by exposing the samples to a Ar-laser, with wavelength of 350nm and 50 mW power density. Sb L-edge XANES measurements have been carried out at LURE (Orsay, France) on the D44 beam line using a Si(111) double crystal monochromator detuned by 60% in order to reject the harmonics. Measurements have been done in TEY (Total Electron Yield) in grazing incidence ( $\approx 5^\circ$ ) in order to collect electronic and structural information on the surface (about 0.6-0.8 $\mu m$ ) of the glasses. Energy calibration has been checked by using a Titanium foil (4966.0 eV) recorded between each glassy sample. Sb- $L_3$  edge (4132 eV) spectra were collected over 340 eV with an energy step of 0.3 eV and counting time of 3s whereas Sb- $L_1$  edge spectra (4698 eV) were recorded over 100 eV with an energy step of 0.3eV and counting time of 1s. For each sample several scans were recorded to improve the signal-to-noise ratio.  $Sb_2O_3$  and  $SbPO_4$  powdering samples deposited onto millipore membranes were recorded in TEY as reference compounds. The absorption background was subtracted from the rough XANES spectra using a linear function. Them spectra were normalised far from the edge in a range of pure atomic absorption (4243.5 eV for Sb- $L_3$  edge and 4774.3 eV for Sb- $L_1$  edge).

## 3. Results

### 3.1. Vitreous domain

Fig. 1 present the vitreous domain of the binary system  $Sb_2O_3$ - $SbPO_4$ . The limits of the glass region were determined using quenching technique.

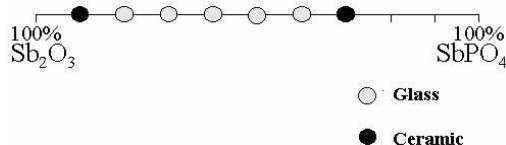


Fig. 1. Vitreous domains of the binary glass system.

### 3.2. Thermal analysis

Table 1 summarizes the characteristics temperatures obtained from DSC curves for the more stable glass composition. We have also included the thermal stability,  $T_x$ - $T_g$ , used as parameter to evaluate the glass stability against devitrification. DSC curves are shown in the Fig. 2 for binary

glasses. From Table1, we can observe an increase in the Tg values as the SbPO<sub>4</sub> concentration increases.

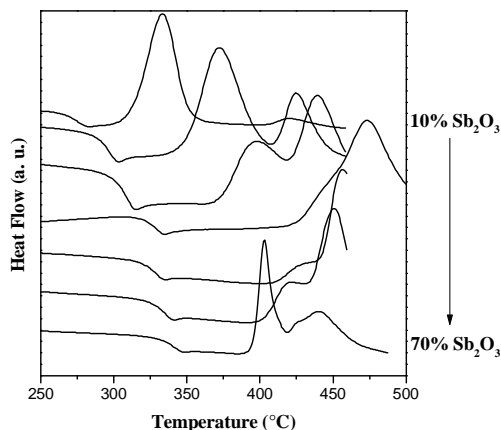


Fig. 2. DSC curves the binary systems.

Table 1. Chemical glass compositions, characteristics temperatures and stability parameter for binary system.

Samples	Glass Compositions (mol %)			Characteristics Temperatures (°C)			Tx-Tg
	Sb <sub>2</sub> O <sub>3</sub>	SbPO <sub>4</sub>	WO <sub>3</sub>	Tg	Tx	Tp	Tx-Tg
Sbp1	90	10	-	265	312	333	47
Sbp2	80	20	-	287	349	373	62
Sbp3	70	30	-	294	372	394	79
Sbp4	60	40	-	317	424	472	107
Sbp5	50	50	-	318	411	457	93
Sbp6	40	60	-	325	400	451	75
Sbp7	30	70	-	334	396	403	62

### 3.3. Optical properties

Optical spectra of these glasses are presented in Fig. 3 from UV to infrared range. Absorption band observed at 3400 cm<sup>-1</sup> can be attributed to stretching, ν of the O-H bonds. The absorption band around 2000 cm<sup>-1</sup> corresponds to multiphonons absorption of the O-P-O bonds, from the antimony orthophosphate. Also, we may note that the band gap of the binary glass appears around 35000 cm<sup>-1</sup> (350 nm).

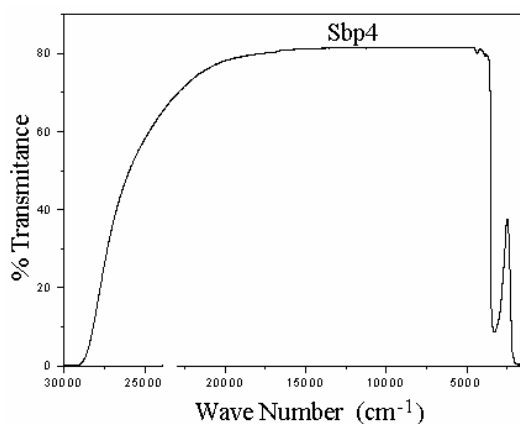


Fig. 3. Optical window in the UV-visible range for the glass compositions Sbp4.

### 3.4. Laser irradiation and XANES data

Sb  $L_3$ -edge data refer to transitions from  $2p_{3/2}$  level towards empty d and s states. The pre-peak in the rising edge ( $\approx 4138$  eV) is attributed to  $2p_{3/2} \rightarrow 5s\sigma^*$  transition whereas the main absorption at higher energy (4145 eV) as interpreted as  $2p_{3/2} \rightarrow 5d$  transition. Correlations between the surface of pre-peak and Sb coordination polyhedron are well established<sup>9</sup>. Roughly speaking a decrease of the pre-peak surface means an increasing mean coordination number for Sb atoms as evidenced on the  $Sb_2O_3$  and  $SbPO_4$ <sup>9</sup>. Sb  $L_1$ -edge data refer to transitions from 2s level towards empty p states. The position of the rising edge is informative of the oxidation state of antimony<sup>10</sup> whereas the intensity of the white line ( $\approx 4704$  eV) and the shape above the white line is strongly dependent on the short and medium range order around Sb. For  $Sb_2O_3$  and  $SbPO_4$  compounds both rising edges are located at the same energy ( $\approx 4702.3$  eV) attesting to the same trivalent state for Sb whereas the general shape is very different due to the different coordination patterns.

During the irradiation by a laser of 50 mW for several hours a change in the coloration of the samples (they pass from yellow to brownish) has been observed but this phenomenon is not permanent and disappears some hours late. Such effect has been long known as photodarkening. We present herein the XANES results obtained on two binary glasses, the Sbp3 and Sbp4 compositions, exposed for 4 and 6 hours, respectively. XANES characterizations on the irradiated Sbp4 sample have been performed immediately after irradiation when the photodarkening is always present, whereas XANES characterizations on the irradiated Sbp3 sample were carried out several days after irradiation. Then the color is turned back to yellow. On the one hand, drastic changes in the shape of both Sb  $L_3$ - and  $L_1$ - edges are observed for the irradiated Sbp4 sample compared to the non-irradiated film as displayed in Figs. 4a and 5a, respectively. According to the above interpretations for the references, the XANES results at the  $L_3$ -edge clearly evidence that a change in the coordination polyhedron of Sb occurs by irradiation. Furthermore, the appearance of a shoulder at  $\approx 3$  eV above the white line at the  $L_1$ -Sb edge could be the evidence of a partial oxidation state change from Sb(III) to Sb(V) upon irradiation. Indeed such energy position is in agreement with the energy of the white line for Sb(V) cations reported in the literature [11]. On the other hand, the structural modifications around Sb after irradiation for the Sbp3 sample, reported in Figs. 4b and 5b, are smaller than those observed on the Sbp4 sample. We note a faint change of the pre-peak intensity at the  $L_3$ -Sb edge after irradiation and some modifications in the shape of the XANES resonances above the white line at the  $L_1$ -Sb edge. Both effects are indicative to small changes of the local and medium order around Sb cations. Furthermore the oxidation state of Sb is always III.

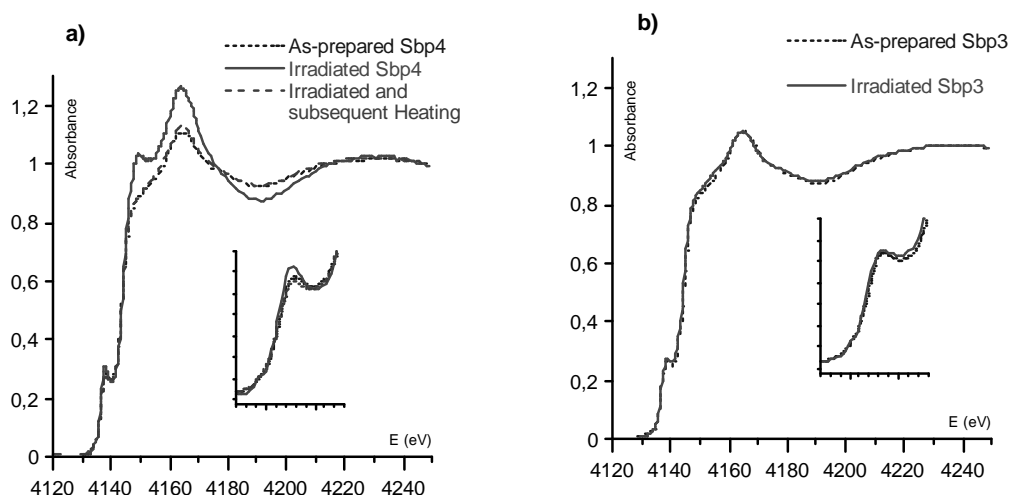


Fig. 4 – XANES spectra recorded at the  $L_3$ -Sb edge for a) Sbp4 and b) Sbp3.

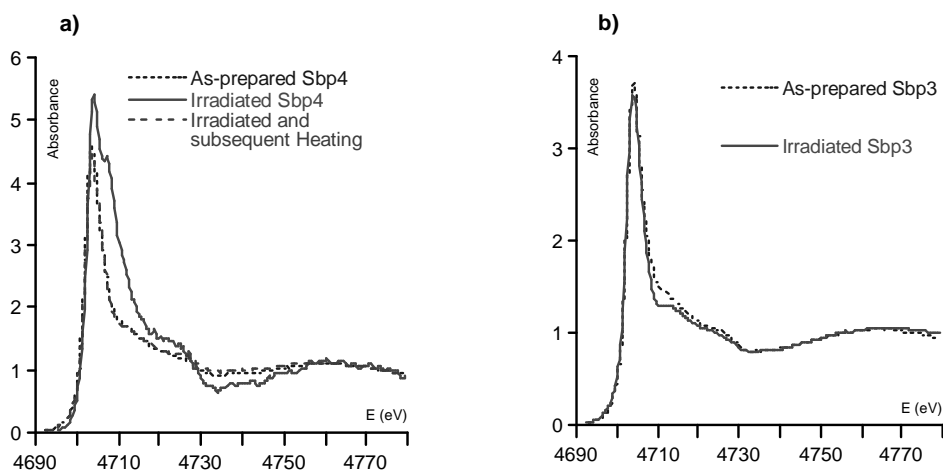


Fig. 5 – XANES spectra recorded at the  $L_1$ -Sb edge for a) SbP4 and b) SbP3.

After the XANES characterizations, the SbP4 sample was immediately heated for 15 hours, in electrical furnace, near  $T_g$ . The XANES spectra recorded after the heat treatment are superimposable to the spectra of the non irradiated sample indicating a reversible character of the photoinduced phenomenon providing that an ad-hoc thermal treatment was carried out.

#### 4. Discussion

Homogenous glasses with higher thermal stability have been obtained with the incorporation of polyphosphates. This may be noted from Table 1 data, which indicate higher value of the difference ( $T_x - T_g$ ) with the incorporation of orthophosphate. This behavior can also be noted from Fig. 1, which indicates a large domain of vitrification in the binary system. It seems that the vitrification is easier with the addition of  $SbPO_4$ , if we assume that isolated  $PO_4$  exist in the glass. The glass transition temperature increases with increase of orthophosphate. This can be linked with the polymerization of the glass network due to the high concentration of  $PO_4^{3-}$  groups. Beside that, both, the temperature of onset of crystallization and the maximum of crystallization values increase from SbP1 to SbP4 (see Table 1).

Samples under irradiation in the wavelength region of the absorption edge with 50 mW power density shown a photodarkening effect. This effect is not permanent and disappears rapidly and glass samples regain its original transmittivity. We have evidenced by XANES measurements on the SbP4 sample that the photodarkening phenomenon induces a breaking of Sb-O bonds in the glassy network: the mean coordination number of Sb in the irradiated film decreases compared to the non-irradiated film. Furthermore, the results at the  $L_1$ -Sb edge suggest also a change in the oxidation state of Sb. The XANES investigation on this sample shows also that the structure is totally restored after heating near  $T_g$ . The XANES results reported for the SbP3 sample strongly indicates that the stronger structural and electronic modifications occur during the photodarkening phenomenon. When the darkening has disappears the oxidation of antimony ions is equal to III as evidenced by the shape of the  $L_1$  white line.

Many publication report studies on the photosensitivity behavior of glasses. Such processes are used for several purposes as light modulators, sun-glasses or glare protection glasses [12,13]. In such glasses the mechanism responsible of the photoinduced effect is related to high concentration of defect centers and a high concentration of vacancies which are caused by considerable local energy absorption. Consequence, these can lead to irreversible as well reversible changes in the structure and some properties as refractive index.

In our case, the structural effect is reversible as shown in Fig. 4 and 5. Annealing in the region of the glass transition temperature restores the  $L_1$  spectra to the original position.

## 5. Conclusion

New photosensitive glasses have been synthesized and characterized in the binary glass system  $\text{Sb}_2\text{O}_3\text{-SbPO}_4$ . We have shown that phosphates increase the thermal stability of the glass samples. Photodarkening effect is observed after irradiation and is not permanent. XANES measurement indicate that the photoinduced effect can be related to defect centers originated by a change on the oxidation number of antimony.

## Acknowledgement

We are fully embedded to D. Graziella (LURE, Orsay) for making the irradiation of the glasses. CNPq and FAPESP are grateful for their financial support.

## References

- [1] M. Ahmed, D.Holland, *Glass Techn.* 28, 41 (1987).
- [2] J. F. Bednarik, J. A. Neely, *Glass techn.Ber.* 55, 126 (1982).
- [3] R. El Mallawany, *J. Mat. Sci: Mat. in Electron.* 6, 1 (1995).
- [4] W. H. Dumbaugh, *Phys. Chem. of Glasses* 19, 121 (1978).
- [5] K. O. Hill, Y. Fujji, D. C. Johnson, B. S. Kawasaschi, *Appl.Phys.Lett.* 32, 647-649 (1978).
- [6] G. Meltz, W. W. Morey, W. H. Glen, *Opt. Ett.* 14, 823-825 (1989).
- [7] K. Y. Raijpure, C. H. Bhosale, *J. Phys. Chem. of Solids*, 61(4), 561-568 (2000).
- [8] F. Vicente, Private communication.
- [9] M. Nalin et al. *J. Non Cryst. Solids* (2001) in press.
- [10] J. M. Durand et al. *J. Non-Cryst. Solids* 194, 109 (1996).
- [11] J. Rockenberger, U. zum Felde, M. Tisher, L. Tröger, M. Haase, H. Weller, *J. Chem. Phys.* 112, 4296 (2000).
- [12] W. Vogel, *Glaschemie*, (1979).
- [13] H. Scholze, *Glass, its nature, structure and properties*, 3<sup>rd</sup> edition, Springer-Verlag, Berlin, 1988.